Journal of Fish Biology
January 2024, Volume 104, Issue 1, Pages 20-33
https://doi.org/10.1111/jfb.15561
https://archimer.ifremer.fr/doc/00853/96456/

Heterogeneity of otolith chemical composition from 2D mapping: relationship with biomineralization mechanisms and implications for microchemistry analyses

De Pontual Hélène [1], MacKenzie Kirsteen [2, *], Tabouret Hélène [3], Daverat Françoise [4], Mahé Kelig [2], Pecheyran Christophe [3], Hüssy Karin [5]

[1] IFREMER DECOD (Ecosystem Dynamics and Sustainability), IFREMER, INRAE, Institut Agro, Centre Bretagne HALGO, LBH, 1625 Route de Sainte Anne du Portzic, CS 10070, 29280 Plouzané, France
[2] IFREMER HMMN, 150 Quai Gambetta, 62200 Boulogne-sur-Mer, France
[3] UMR 5254, Université de Pau et des Pays de l'Adour (UPPA), Avenue de l'Université, BP 576 - 64012 Pau Cedex, France
[4] INRAE, 173 Route de Saint-Jean-de-Luz, 64310 Saint-Pée-sur-Nivelle, France
[5] National Institute of Aquatic Resources, Section for Oceans and Arctic, Technical University of Denmark, Kemitorvet, Building 201, 2800 Kongens Lyngby, Denmark

* Corresponding author : Kirsteen MacKenzie, email address : kirsteen.mackenzie@ifremer.fr

Abstract :

Although otoliths are widely used as archives to infer life history traits and habitat use in fishes, their biomineralization process remains poorly understood. This lack of knowledge is problematic as it can lead to misinterpretation of the different types of signals (e.g. optical or chemical) that provide basic data for research in fish ecology, fisheries management and species conservation. Otolith calcification relies on a complex system involving a pericrystalline fluid, the endolymph, which organic and inorganic compositions are spatially heterogeneous for some constituents. This property stems from the particular structure of the calcifying saccular epithelium. In this study, we explored the spatial heterogeneity of elemental incorporation in otoliths for two species of high economic interest, European hake Merluccius merluccius (L. 1758) and European sea bass Dicentrarchus labrax (L. 1758). Two-dimensional mappings of chemical elements were obtained by UV-fs LA-HR-ICPMS analyses on transverse sections of sagittae. Results highlighted a clear asymmetry between proximal (sulcus) and distal (antisulcus) concentrations for elements such as magnesium Mg, phosphorus P, manganese Mn and potassium K with concentration gradient directions that varied depending on the element. Strontium Sr and barium Ba did not show a proximo-distal gradient. These results are discussed in the light of current knowledge on the endolymph composition and the mechanisms that lead to its compartmentalization, highlighting the need for further research on otolith biomineralization. Operational implications for studies based on otolith chemical composition are also discussed with emphasis on advice for sampling strategies in order to avoid analytical biases, and the need for in-depth analyses of analytical settings before comparing otolith signatures between species or geographical areas.

Keywords : Endolymph, European sea bass, European hake, saccular epithelium, spatial pattern, trace elements

Funding Information

This research was conducted in the framework of the BARFRAY project (2017-2020 funded by the European Maritime and Fisheries Funded EMFF- OSIRIS N°: PFEA 400017DM0720006, the French Ministry of Agriculture and Food, France Filière Pêche and IFREMER) and the AHA project (2018-2020, funded by EU DG-MARE, EASME/EMFF/2016/1.3.2.7/SI2.762036).

Introduction

Otoliths, also called earstones, are paired concretions of calcium carbonate in the fish inner ear. They play a vital role in fish life, as they are involved in the balance and hearing systems. They develop throughout the life of the fish through an incremental accretion process that is regulated by different rhythms (daily, lunar, seasonal) and fluctuates according to endogenous (ontogeny, physiology) and exogenous (e.g. hydroclimatic and trophic conditions) drivers. Unlike scales, which can act as calcium and phosphorus reservoirs (Vieira *et al.*, 2011), otoliths remain stable over time, only exceptionally undergoing processes of remodeling or resorption (Mugiya and Uchimura, 1989). These properties give otoliths unique potential for the reconstruction of both environmental parameters and fish life traits at various temporal resolutions. Of the three pairs of otoliths that exist in the vestibular system of teleost fish, the largest are termed *sagittae* (hereinafter be referred to as otoliths), the corresponding end organs being the saccules (see e.g. Panfili *et al.*, 2002; Schulz-Mirbach *et al.*, 2019 for detailed schemes of fish inner ear anatomy).

While otolith optical patterns (micro- and macro-increments) have long been used to estimate life traits such as age and growth, the use of chemical signals emerged more recently and has rapidly grown since the 1990s, in parallel with technological advances in the field of biogeochemistry (see e.g. the review by Walther, 2019) . Applications are endless and cover inferences at various scales: 1) individual (life traits, habitat use and migratory behaviors, physiological state, etc.); 2) population (by aggregating individual data) and 3) ecosystem (for e.g. experienced temperatures and paleoclimate reconstruction). Regardless of the power of this tool, however, it must be used with caution, as its biomineralization processes are still very imperfectly understood. This knowledge gap can lead to misinterpretation of chemical data, with serious consequences for the inferences drawn (Sturrock *et al.*, 2014).

Briefly, biomineralization results from the implementation of dynamic physiological processes, which are specific and complex and controlled by gene expression. Unlike many other

biominerals, the otolith formation occurs in an acellular medium, the endolymph, which is secreted by the saccular epithelium. As a consequence, the biomineralization process strictly depends on the endolymph chemistry (Payan *et al.*, 2004). Whereas the saccular epithelium has to provide all the calcification precursors, through the active or passive transport of ionic precursors as well as the synthesis of organic components, the ultimate biomineralization process occurs at the interface between the otolith and endolymph. It is largely acknowledged that crystallization is driven by organic macromolecules that either form the organic matrix on which CaCO3 precipitates or that regulate the precipitation itself. Thomas and Swearer (2019) provided an overview of the latest knowledge on proteins identified in the endolymph and the otolith of different fish species. Moreover, a proteomic approach recently identified more than 380 proteins in the otolith/endolymph of black bream *Acanthopagrus butcheri* (Munro 1949) (Thomas *et al.*, 2019) and provided a new basis to understand the mechanisms of diel rhythm of accretion and regulation of ionic transfer into the endolymph. Mechanisms of trace element incorporation, by substitution for Ca, by protein binding, or by trapping in the crystalline structure, depend on the element under consideration and give that element environmental and/or physiological tracer properties (Hüssy *et al.*, 2021). Although these advances constitute breakthroughs in the understanding of biomineralization mechanisms, they do not account for the spatial dimension of the mechanisms that give the otolith its three-dimensional shape and chemical composition.

The use of elements with spatially heterogeneous incorporation are a challenge for applications of otolith microchemistry, where measurements are typically carried out as 1D measurements (e.g. transects or spots) without assessment of whether the element assay is performed in an area where the element is poorly incorporated and therefore difficult to quantify. Moreover, standardising the location of measurements would be required for such elements, both between

individuals in a given study and between studies when comparisons are made (e.g. meta-analysis).

This question was addressed in this study by carrying out two-dimensional elemental mapping in order to investigate the spatial distribution of the elements in the otolith. We aimed at: 1) defining, among elements that are commonly analyzed, those with a spatially heterogeneous incorporation pattern, 2) establishing whether this heterogeneity is species-specific and, 3) reviewing the literature for potential biomineralization mechanisms leading to such heterogeneity.

Two species of marine round fish, European hake *Merluccius merluccius* (L. 1758) and European sea bass *Dicentrarchus labrax* (L. 1758), were used in this study. European hake are amongst the most important commercial demersal species in Northeast Atlantic Ocean, with a population extending from the North African coast to the Norwegian Sea, from coastal zones to continental shelves, and from around 20 to 200 m depth with potential homing behavior to foraging areas (de Pontual *et al.*, 2012, 2013; Staby *et al.*, 2018). In the Northeast Atlantic, hake are likely split into northern (from southern France northwards) and southern (from northern Spain southwards) stocks, although with likely movements between stocks (Tanner *et al.*, 2012). In the Bay of Biscay, there may be adult movement towards spawning areas along the shelf break in winter (Alvarez *et al.*, 2001; Poulard, 2001). European sea bass is also a highly commercially valuable species, with its Northeast Atlantic range extending from the Canary Islands and Morocco to Scandinavia and from estuaries and coastal lagoons to open sea areas, occupying waters between the surface and over 230 m (de Pontual *et al.*, 2023), with much broader temperature and salinity ranges than European hake. Adult sea bass perform westward spawning migrations in autumn-winter to largely offshore spawning areas and return migrations to feeding areas in spring to early summer with a high degree of fidelity to both spawning and feeding areas (Le Luherne *et al.*, 2022; de Pontual *et al.*, 2023). Nursery areas for European sea

bass are inshore, and can be in lagoons, estuaries and fjords with associated changes in temperature and salinity, where juveniles stay until they reach maturity (Pawson & Pickett, 1996; López *et al.*, 2015).

Material and methods

Analyses were carried out on otolith of two species of round fish, European hake *Merluccius merluccius* (L. 1758) and European sea bass *Dicentrarchus labrax* (L. 1758). Four hake and three sea bass (details in Table 1) were used in this study, provided to Ifremer following tag return campaigns (see de Pontual *et al.*, 2013, 2023 for full details and further associated data).

Table 1. *Details of European hake Merluccius merluccius and European sea bass Dicentrarchus labrax individuals sampled in this study.*

Species	ID	Sex	Total length (cm)
M. merluccius	M5-M123	F	45.2
M. merluccius	M5-M127	M	44.8
M. merluccius	M4-M62	F	46.0
M. merluccius	M5-M128	F	49.0
D. labrax	A10780	M	66.5
D. labrax	A10782	F	67.0
D. labrax	A11922	M	54.8

Otolith collections

Otoliths of European hake were sourced from collections held by Ifremer in the framework of the intensive conventional tagging program, which ran from 2002-2007 in the Bay of Biscay (de Pontual *et al.*, 2013)

Otoliths of European sea bass were sourced from collections held by Ifremer in the framework of the DST (Data Storage Tags) tagging program in the Southern North Sea, the English Channel and the Bay of Biscay from 2013-2017 (de Pontual *et al.*, 2023).

For both species, otolith sections were prepared in the transverse plane through the core. This section plane is particularly suitable because it covers the entire life of the fish, and comprises the proximal (facing the macula) and distal areas of the otolith. The sections were obtained by following a classical preparation protocol, namely: 1) embedding in a chemically neutral epoxy resin, 2) sectioning in the transverse plane, and 3) grinding and polishing through the core.

For standardization, left otoliths were systematically used for trace element analysis. All otolith sections were imaged under transmitted and reflected light prior to subsequent analysis.

Decontamination was performed by a fast laser preablation during which no measurements were taken.

ICP-MS analysis

The elemental composition of otoliths was quantified using a UV high-repetition-rate femtosecond laser ablation (fs-LA) system (Lambda III, Nexeya SA/Amplitude Systèmes, Canejan, France) coupled to a High Resolution Inductively Coupled Plasma Sector Field Mass Spectrometer (HR-ICP-SFMS, XR, Thermo Scientific, USA) at the IPREM (Institute of Analytical Sciences and Physico-Chemistry for Environment and Materials, Pau, France).

The two dimensional elemental mapping consisted of ablating the whole surface of the otolith through a series of successive single scans, producing an elemental image of each transverse section. The ablation was performed at 200 Hz with a 13 µm beam diameter according to the operating conditions (described in Supporting information: Table 1).

We tested different laser platine speeds to optimize the spatial resolution given by the final pixel size: 3 individuals were analyzed with an 18 $\mu m.s^{-1}$ speed, 1 otolith with a 10 $\mu m.s^{-1}$ speed and three with a 5 $\mu m.s^{-1}$ speed. In order to avoid image distortion, all the images presented in this study were

homogenized thanks to bilinear interpolation on ImageJ software (Rueden *et al.*, 2017) resulting in a 20x20 µm square pixel resolution, and all were of sufficiently high resolution to clearly determine patterns of elemental distribution across the otoliths studied here. The surface of each section was cleaned prior to analysis using a fast pre-ablation strategy at 9 KHz and 5 $mm.s^{-1}$ (Wyndham *et al.*, 2004). The analysis of two certified reference glasses NIST612 and NIST610 (National Institute of Standards and Technology, USA) ensured accurate analysis. Calcium was used as an internal standard to account for any variation in the amount of ablated material and laser energy in the ablation yield. Analytical accuracy was measured with the fish certified otolith reference material FEBS-1 (National Research Council Canada, Canada). Ten isotopes were analyzed in all the samples (^{7}Li, ^{23}Na, ^{25}Mg, ^{31}P, ^{39}K, ^{55}Mn, ^{63}Cu, ^{85}Rb, ^{88}Sr, ^{138}Ba, ^{43}Ca) and the distribution of ^{66}Zn, ^{89}Y and ^{139}La was examined in at least one individual. Since these three isotopes were below the detection limits, we did not keep them for the next steps of the analysis. The average detection limits were calculated on three standard deviations of the blank gas: ^{7}Li: 48.7 $ng.g^{-1}$, ^{23}Na: 2826.6 $ng.g^{-1}$, ^{25}Mg: 23.7 $ng.g^{-1}$, ^{31}P: 502.7 $ng.g^{-1}$, ^{39}K: 160.2 $ng.g^{-1}$, ^{55}Mn: 25.9 $ng.g^{-1}$, ^{63}Cu: 21.5 $ng.g^{-1}$, ^{85}Rb: 14.1 $ng.g^{-1}$, ^{88}Sr: 20.3 $ng.g^{-1}$, ^{138}Ba: 2.6 $ng.g^{-1}$. Accepted recovery of reference materials ranged from 93% to 110%. Element compositions were expressed as mass elemental ratios (element:Ca) on the basis of the stoichiometry of Ca carbonate (380,000 $\mu gCa.g^{-1}$ otolith) (Campana, 1999). Data were processed using a VBA Macro and exported to ImageJ software (Rueden *et al.*, 2017) to generate images of element:Ca ratios.

No attempt to differentiate element mapping by sex or size was made due to the low number of otoliths analysed for each species.

Ethical statement

The fishes sampled here for otoliths were part of tag-recapture studies, under permits from the French Research Minister. Tagged and recaptured fish were dead when provided to Ifremer by fishers and members of the public, and thus no permits were required for the present study.

Results

Regardless of the otoliths analyzed, the 2D elemental maps showed different spatial patterns, depending on the element considered but with patterns that were consistent across otoliths for each element respectively. Three groups were observed: 1) elements that did not show spatial heterogeneity, 2) elements with higher concentration on the proximal side (i.e. sulcus side, facing the macula) than on the distal side (anti sulcus side) and 3) elements with higher concentration on the distal side.

European hake

For European hake, the 2D maps with the highest spatial resolution are presented in Fig. 1. Strontium and Ba appear to be homogenously distributed on the proximo-distal axis. Magnesium and Mn (subsequently referred to as "distal+ elements") present higher concentrations on the distal side compared to the proximal one. The opposite is observed for P and, to a lesser extent, for K (subsequently referred to as "proximal+ elements").

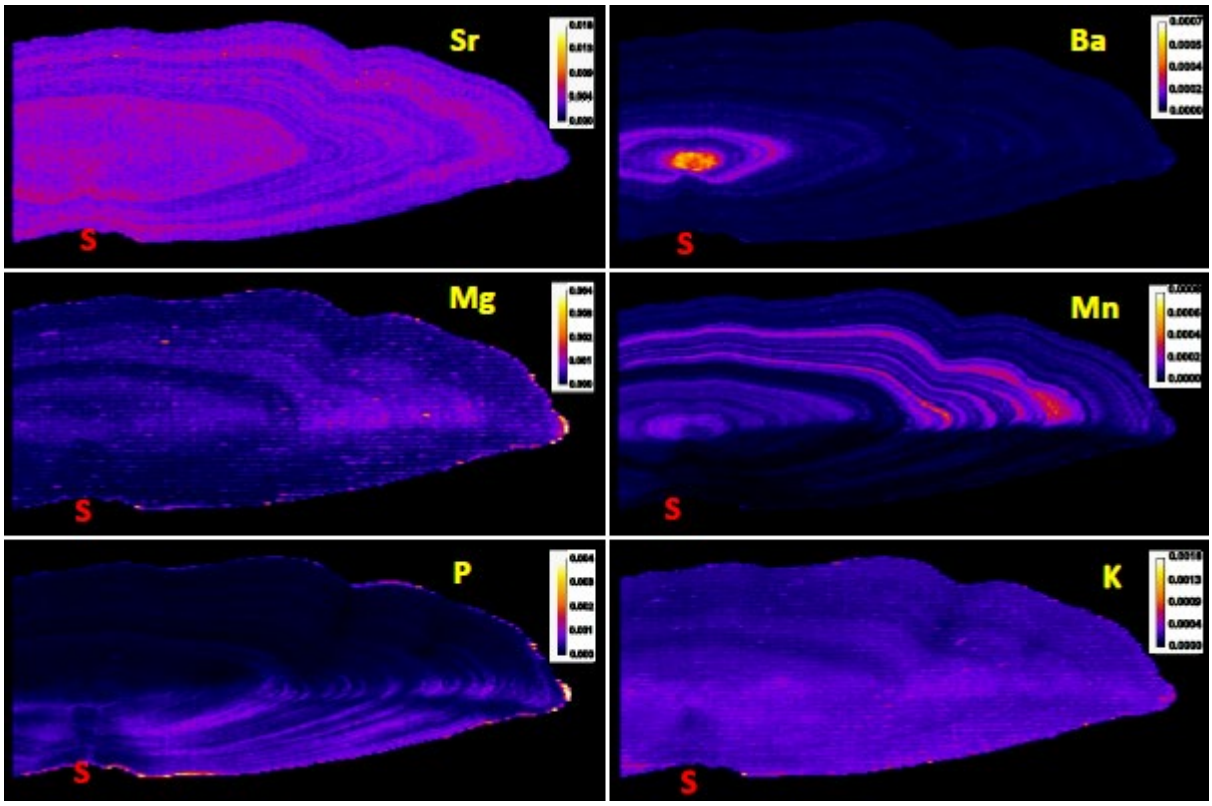

Figure 1. *High spatial resolution acquisition. Transverse section of a European hake Merluccius merluccius otolith (ID M5-M123, ventral side, sulcus (S) down) showing different spatial patterns of element-Ca ratios: 1) Sr and Ba are homogenously distributed (top panels), 2) Mg and Mn (distal+ elements) have higher concentrations on the distal (antisulcus) side (middle panels) and, 3) P and K (proximal + elements) show higher concentrations on the proximal (sulcus) side (bottom panels). Color scales represent element:Ca concentration and have been standardized across all otoliths for each ratio.*

While Sr:Ca and Ba:Ca do not show proximo-distal differences (Fig. 1), the observed spatial heterogeneity in element concentrations seems to be consistent across individuals of European hake for both Mn and Mg (Fig. 2), and P and K (Fig. 3).

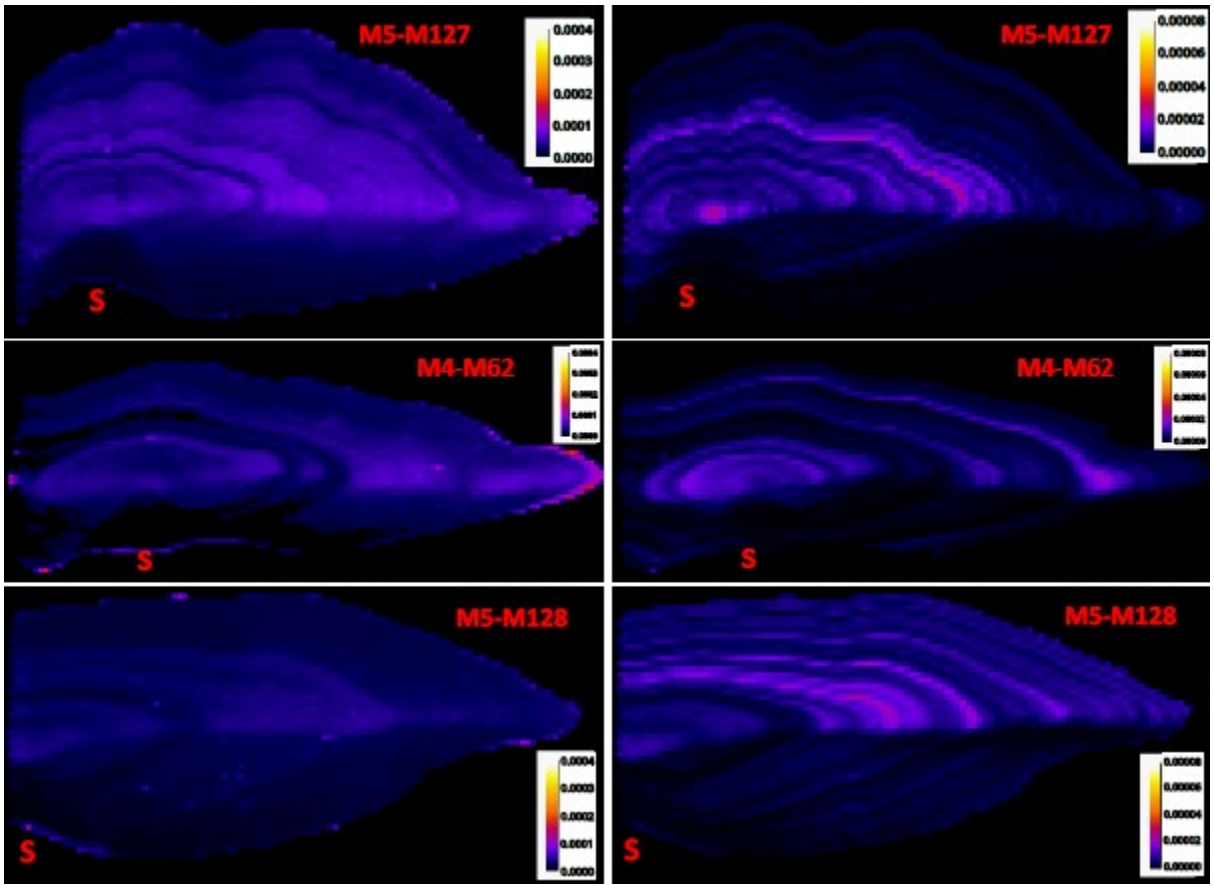

Figure 2. *Transverse sections of European hake Merluccius merluccius otoliths (ID number on the images, ventral side, sulcus (S) down). 2D maps of "distal+" elements: Mg (left panels) and Mn (right panels). Color scales represent element:Ca concentrations normalized across individuals for a given element.*

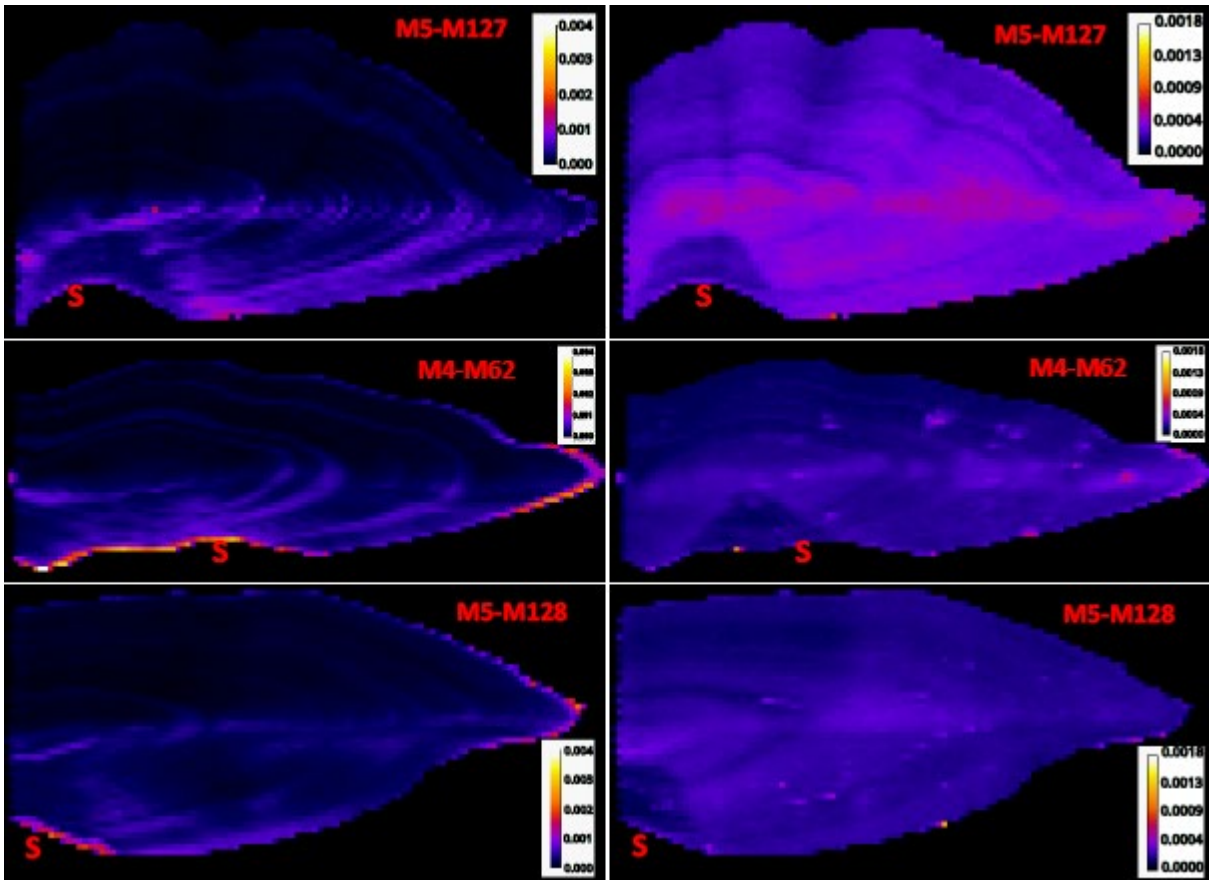

Figure 3*. Transverse sections of European hake Merluccius merluccius otoliths (ID number on the images, ventral side, sulcus (S) down). 2D maps of "proximal+" elements that are more concentrated on the proximal side: P (left panels) and K (right panels). Color scales represent element:Ca concentrations normalized between individuals for a given element.*

European sea bass

In European sea bass, otolith 2D maps of Sr:Ca and Ba:Ca ratios do not show any proximo-distal gradient (Fig. 4) whereas proximo-distal properties are identical to those of European hake otoliths: Mg and Mn are "distal+ elements" (Fig. 5), and P and K are "proximal+ elements" (Fig. 6).

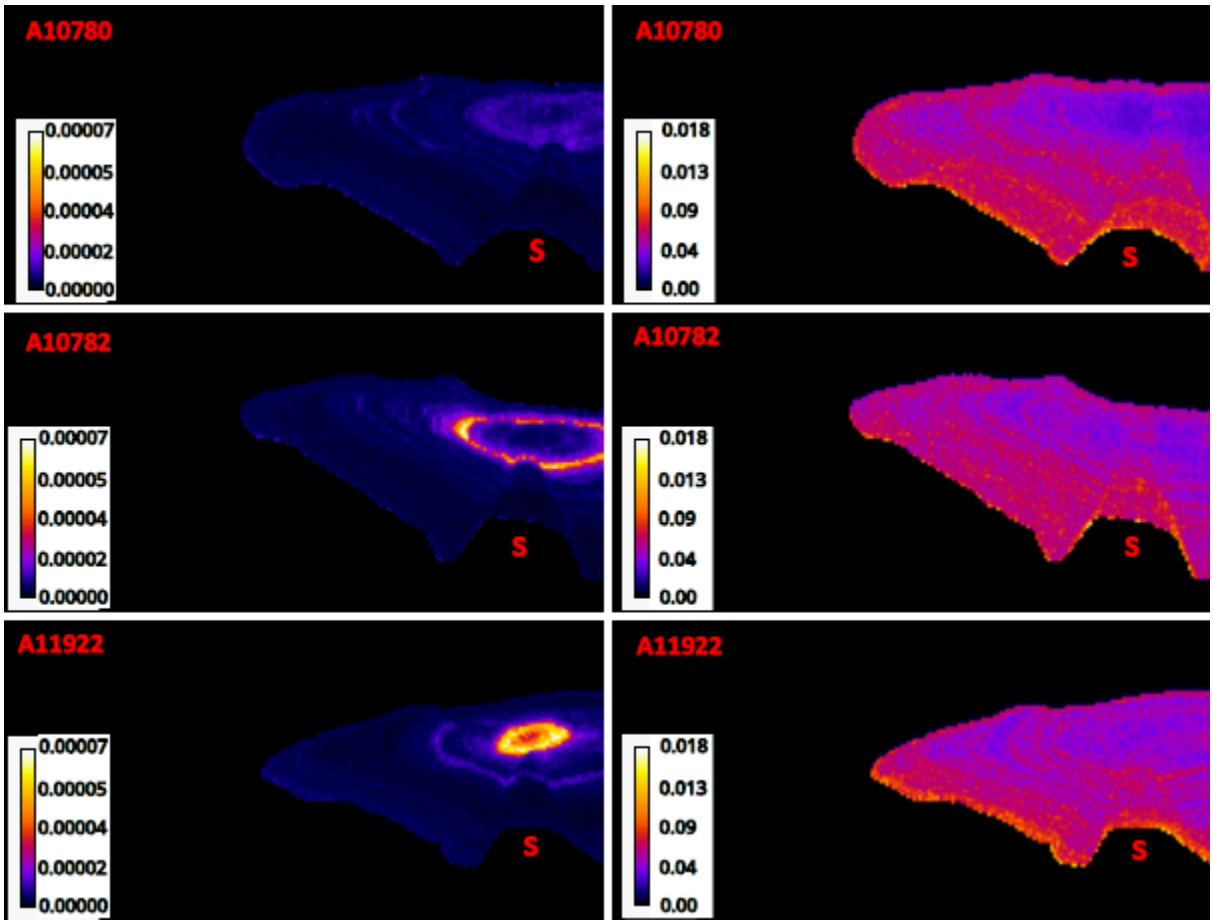

Figure 4. *Transverse sections of European sea bass Dicentrarchus labrax otoliths (ID number on the images, ventral side, sulcus (S) down). 2D maps of Ba (left panels) and Sr (right panels) concentrations. Color scales represent element:Ca concentrations normalized between individuals for a given element.*

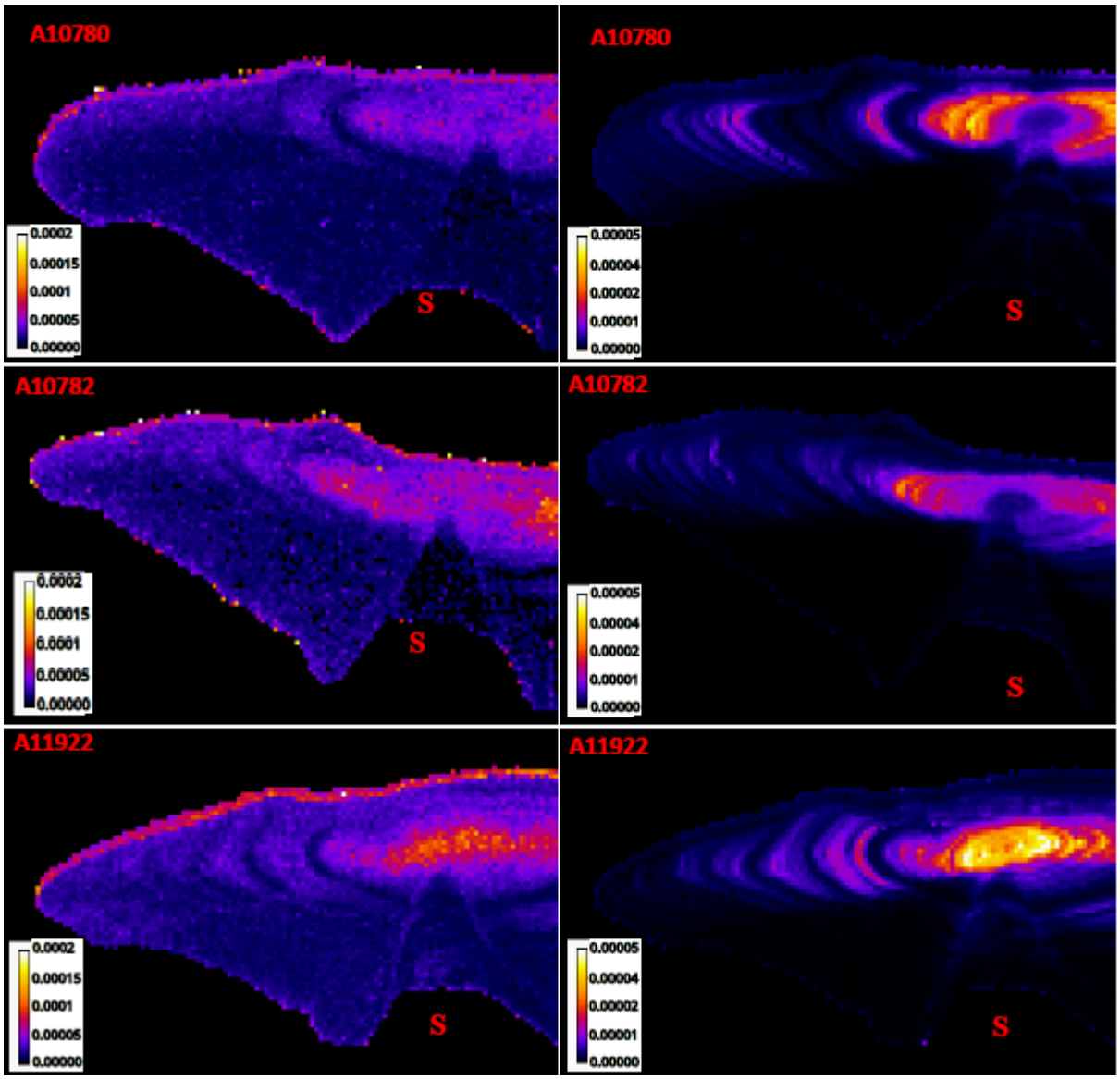

Figure 5. *Transverse sections of European sea bass Dicentrarchus labrax otoliths (ID number on the images, ventral side, sulcus (S) down). 2D maps of "distal+" elements: Mg (left panels) and Mn (right panels). Color scales represent element:Ca concentrations normalized between individuals for a given element.*

While Sr:Ca and Ba:Ca do not show proximo-distal differences (Fig. 4), the observed spatial heterogeneity in element concentrations seems to be consistent across individuals of European sea bass for both Mn and Mg (Fig. 5), and P and K (Fig. 6), as in European hake.

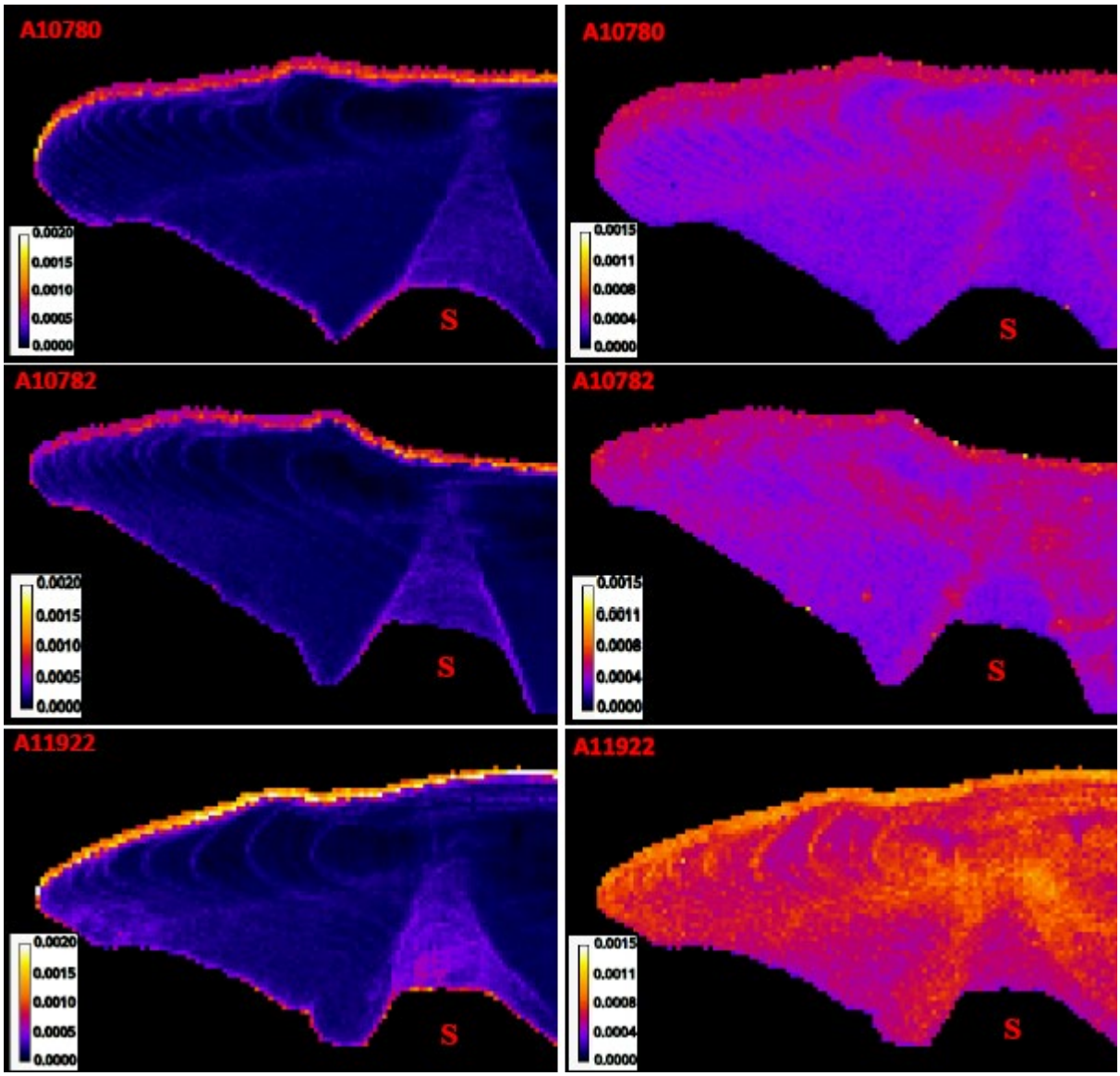

***Figure 6**. Transverse sections of European sea bass Dicentrarchus labrax otoliths (ID number on the images, ventral side, sulcus (S) down). 2D maps of "proximal+" elements: P (left panels) and K (right panels). Color scales represent element:Ca concentrations normalized between individuals for a given element.*

It is worth noting that these chemical proximo-distal gradients are maintained in an equivalent way (and notably in the same direction) for both species, although there are differential accretion rates on this axis for both species. Indeed the images (Fig. 2-6) show that the nucleus is close to the proximal side in hake while it is clearly shifted towards the distal side in sea bass which reflect some differences in the biomineralization process.

More globally, we also note that these 2D images reveal the potential of certain chemical elements as chronological structures or chemical clocks. This is particularly visible for e.g. phosphorus on sea bass otoliths (Fig. 6).

Discussion

Heterogeneity: is it element dependent, species dependent?

Research based on chemical images of otoliths is still relatively scarce because of various constraints (time/cost analysis, instrumental stability, etc.). Nevertheless, a certain number of 2D elemental maps are available in the literature and show, to different degrees, spatial heterogeneities in the distribution of some elements. For instance, Mn, Br, and Zn (Limburg *et al.*, 2011; Limburg *et al.*, 2015; Limburg and Elfman, 2017) as well as Mg and P (Hüssy *et al.*, 2021) show asymmetrical concentrations between the proximal and distal faces of the otoliths across different species. The direction of this asymmetry (proximal+ or distal+), when it exists, clearly depends on the element considered. At first glance, the direction is generic (constant across species) and thus most probably proceeds from fundamental processes of the biomineralization of the otolith. The architecture of the saccular epithelium, the mechanisms of ion transport and matrix synthesis, and the spatial heterogeneity of the composition of the endolymph, both organic and mineral, are all systemic processes that drive these patterns. The review of these processes allows us to address specific hypotheses and to identify research needed for a better understanding of the functioning of the sacculus/endolymph/otolith complex.

Saccular structure, ion transport and matrix synthesis

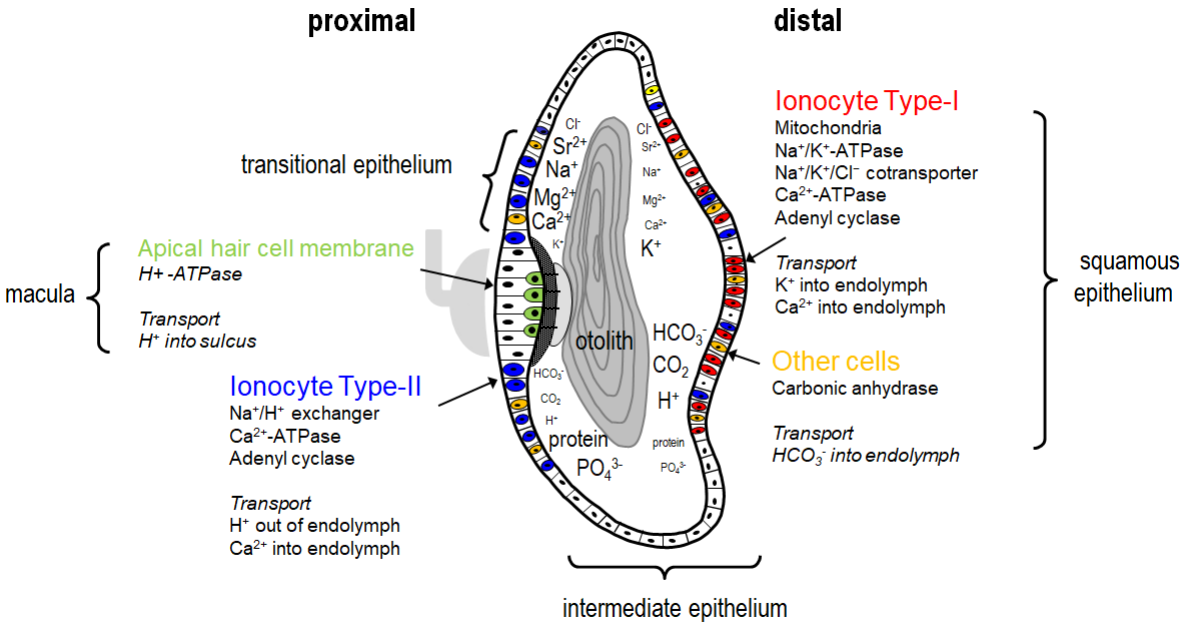

Figure 7: Schematic model of a cross section across an otolith, and the architecture of the saccular epithelium, representing different cell types and their spatial distribution patterns within the epithelium (modified from Hüssy (2021), based on (MayerGostan, 1997; Pisam *et al.*, 1998; Payan *et al.*, 1999; Takagi and Takahashi, 1999; Edeyer *et al.*, 2000; Payan *et al.*, 2002; Borelli *et al.*, 2003; Beier *et al.*, 2004; Payan *et al.*, 2004; Shiao *et al.*, 2005; Kwan *et al.*, 2020). The sulcus of the otolith is the part of the otolith overlaying the macula.

Aragonite crystal growth requires the simultaneous presence of Ca^{2+} and CO_3^{2-} in the endolymph, which requires active or passive transport from the blood plasma across the saccular tissue. The saccular tissue is a monolayer epithelium (except for the macula) consisting of different highly specialized cells. Prominent among these are the so called ionocytes, which are responsible for the transport of ions into the endolymph. The squamous epithelium on the distal side of the otolith (opposite the macula) contains patches of smaller ionocytes (Type I and Type II) (Fig. 7), the transitional epithelium surrounding the macula contains exclusively large ionocytes (Type II) grouped in a dense meshwork, while the intermediate epithelium does not contain ionocytes (MayerGostan, 1997; Pisam *et al.*, 1998; Kwan *et al.*, 2020). The smaller Type I ionocytes on the distal side contain predominantly Na^+/K^+-ATPase, $Na^+/K^+/Cl^-$ cotransporter and Ca^{2+}-ATPase. In addition, they are rich in mitochondria and adenyl cyclase. The role of these ionocytes is to maintain an ionic gradient across the epithelium by pumping K^+ and Ca^{2+} into the endolymph (MayerGostan, 1997; Takagi, 1997; Kwan *et al.*, 2020). The

large Type II ionocytes in the transitional epithelium surrounding the macula are rich in Na^+/H^+ exchanger and Ca^{2+}-ATPase (Tohse *et al.*, 2004; Kwan *et al.*, 2020) that ensure transport of Ca^{2+} into and H^+ out of the endolymph. Contrary to Kwan et al. (2020), Takagi (1997) also observed Na^+/K^+-ATPase activity in the transitional epithelium. It is not clear whether this discrepancy is related to species-specific differences in sacculus structure (Takagi, 1997: *Oncorhynchus mykiss* (Walbaum 1792); Kwan *et al.*, 2020: *Scomber japonicus* Houttuyn 1782), or to methodological differences in sample preparation. In both areas, cells rich in carbonic anhydrase, the enzyme catalysing the interconversion between CO_2 and water and the dissociated ions of HCO_3^- and H^+, are present (Tohse *et al.*, 2004; Beier *et al.*, 2006; Kwan *et al.*, 2020). In addition to the active transport involving Ca^{2+}-ATPase, Ca^{2+} can also enter the endolymph through passive paracellular diffusion across the sacculus on the proximal side of the otolith (Tohse and Mugiya, 2001; Payan *et al.*, 2002; Cruz *et al.*, 2009). The apical hair cells of the macula contain H^+-ATPase that secretes H^+ into the sulcus, thereby preventing biomineralization in the sensory macula (Shiao *et al.*, 2005).

In addition to $CaCO_3$, otoliths also contain c. 2% organic components, which are synthesized in the saccular epithelium. Synthesis of collagen, which makes up 45 - 85 % of the otolith organic matrix (Baba *et al.*, 1991; Asano and Mugiya, 1993; Sasagawa and Mugiya, 1996), occurs primarily in the transitional epithelium on the proximal side of the otolith (Murayama *et al.*, 2004). The synthesis of a number of other organic matrix components, among those the Ca-binding glycoproteins that have a structural function by stabilizing the matrix (Asano and Mugiya, 1993), is restricted to the outer margins of the transitional epithelium (Takagi and Takahashi, 1999; Weigele *et al.*, 2015) and the squamous epithelium (Takagi and Takahashi, 1999). Collagenous matrix proteins occur throughout the otolith but with highest concentrations on the proximal side where they are synthesized (Takagi and Takahashi, 1999; Murayama *et al.*, 2004). The Ca-binding glycoproteins are primarily found along the otoliths' longest growth

axes (Takagi and Takahashi, 1999), i.e. in the interphase between proximal and distal sides of the epithelium.

As a result of the spatial heterogeneity in ionocyte activity, endolymph composition is not homogenous throughout the endolymph. On the distal side of the otolith, concentrations of K^+, total CO_2, HCO_3^-, and H^+ are higher, while Ca^{2+} concentrations are higher on the proximal side (Payan *et al.*, 1999; Edeyer *et al.*, 2000; Payan *et al.*, 2002; Borelli *et al.*, 2003; Payan *et al.*, 2004). There is only sporadic information on transport of other elements. Payan *et al.* (2002) showed in vitro that movement of Sr^{2+} across the endolymphatic epithelium is passive and occurs primarily on the proximal side of the otolith. Assuming similar passive transport of other elements seems reasonable, given the similar proximal/distal concentration patterns with higher concentrations of Sr^{2+}, Na^+, and Mg^{2+} in the proximal endolymph (Payan *et al.*, 1999; Payan *et al.*, 2002; Payan *et al.*, 2004). Higher concentrations of protein and PO_4^{3-} in the proximal endolymph (Payan *et al.*, 1999; Edeyer *et al.*, 2000; Borelli *et al.*, 2003; Payan *et al.*, 2004) are also consistent with highest matrix synthesis activity in the transitional epithelium.

Element occurrence in the crystal lattice

An additional issue to consider in the context of spatial heterogeneity in otolith element concentration is where in the growing crystal structure they occur. Elements can be incorporated into the otolith through the following mechanisms: 1) randomly trapped in the crystal lattice, 2) substituted for Ca on the growing crystal surface, or 3) bound to organic matrix constituents. Sr^{2+}, Ba^{2+}, and Mn^{2+} substitute for Ca^{2+} (Doubleday *et al.*, 2014; Thomas *et al.*, 2017), while a number of other elements (Mg^{2+}, Li^+, K^+, Rb^+, Al^+, Pb^+, Cd^+, Fe^{2+}) are likely randomly trapped in the crystal lattice (Miller *et al.*, 2006; Izzo *et al.*, 2016; Thomas *et al.*, 2017). One would

therefore expect, that the concentration of these elements in the endolymph is reflected in the otolith.

Matrix-bound elements that are co-factors in many enzymes and proteins include Cu, Zn (Miller *et al.*, 2006; Izzo *et al.*, 2016; Thomas *et al.*, 2017), Fe and Mn (Izzo *et al.*, 2016), as well as Co, Ni and P (Thomas *et al.*, 2017). A recent review by Hüssy *et al*. (2021) highlights that Mg^{2+} and Mn^{2+} seem to occur as substitutes for Ca or randomly trapped, and can be bound to the organic matrix, and may therefore exhibit spatial patterns associated with all incorporation mechanisms.

Hypotheses: Patterns of heterogeneity

In the following, we compare the patterns observed in the present study and in published 2D element maps with hypotheses to examine to what extent spatial heterogeneity is a generic feature of element incorporation. Combining information on the sacculus cellular structure with patterns of ionocyte types and activity and binding sites of elements in the growing crystal lattice, we propose the following hypotheses for spatial element patterns:

Elements substituting for Ca/randomly trapped: Otolith concentrations of Ca^{2+}, Sr^{2+},Na^{+}, and Mg^{2+} are hypothesized to be higher in the proximal than the distal side as these are primarily secreted from the proximal area of the saccular epithelium (Fig. 7). Other elements that may be expected to follow the same pattern are Ba^{2+}, Mn^{2+}, Li^{+}, Rb^{+}, Al^{+}, Pb^{+}, Cd^{+}, and Fe^{2+}, providing that they primarily enter the endolymph on the proximal side of the epithelium. The concentration of K^{+} on the other hand, is hypothesized to be higher on the distal side.

Substitutes for Ca^{2+}: In the present study we found that Sr^{2+} and Ba^{2+} were homogenously distributed around the otolith for both hake and sea bass. Only few studies with 2D elemental maps of suitable otolith sections exist for comparison with the present results. In the majority of these, Sr^{2+} and Ba^{2+} are homogenously distributed around the otolith in *Arapaima* sp. Müller

1843 (Limburg and Elfman, 2017; Hüssy *et al.*, 2021), *Brachymystax lenok* (Pallas 1773) (Prohaska *et al.*, 2016), *Ictalurus punctatus* (Rafinesque 1818), *Catostomus commersonii* (Lacepède 1803) (Limburg *et al.*, 2010, Sr2+ only), *Perca flavescens* (Mitchill 1814) (Collingsworth *et al.*, 2010, 2010, Sr2+ only) and *Platycephalus bassensis* Cuvier 1829 (McFadden *et al.*, 2016); but apparently slightly higher in the proximal side of the otolith in *Sander vitreus* (Mitchill 1818) (Limburg *et al.*, 2010) and *Gadus morhua* L. 1758 (Limburg *et al.*, 2011; Limburg and Elfman, 2017; Heimbrand *et al.*, 2020; Hüssy *et al.*, 2021). It thus appears that the near-homogenous Sr and Ba proximal-distal distributions observed in the present study are a generic pattern, which differs from our hypothesis. The most likely explanation for this discrepancy may be attributable to the fact that spatial measurements of endolymph Sr and Ba is often measured as protein-bound complex and not as free ions, while it is the free ions that are incorporated into the otolith crystal lattice.

Randomly trapped: To our knowledge, the present study is the first publication of 2D maps of otolith K^+. These maps showed highest concentration of K^+ on the proximal side of the otolith in both hake and sea bass, although this distribution was more evident in hake. Otolith K^+ was expected to mirror the higher K^+ in the distal endolymph. One explanation for this apparent contradiction could be that the spatial measurements of K (and Na) in the endolymph were made by flame photometry (Payan *et al.*, 1999) and therefore do not necessarily reflect the free ion concentration likely to be randomly trapped in the otolith. Another hypothesis could be that of differential incorporation into the organic matrix of the otolith, depending on the species. It can be noted, for example, that the "Proximal+" character is questionable on sea bass otoliths with high K concentrations throughout the distal side (Fig. 6); in agreement with the measurements made in the endolymph on the turbot). Another argument in favour of a protein-bound incorporation in the otolith is the fact that these elements appear to show temporally

varying concentrations throughout the fish life, the periodicity of which remains to be established.

Protein-bound: Otolith concentrations of P, Cu, and Zn are hypothesized to be highest along the longest growth axis and in the proximal side of the otolith. In the present study we found higher concentrations of P^{+} throughout the proximal side of the otolith, particularly in hake. Only a few studies show maps of P, and concentrations of P in these are generally highest along the dorso/ventral growth axis and towards the distal side of the otolith (Heimbrand *et al.*, 2020; Hüssy *et al.*, 2021) as are other protein-bound elements like Zn (Limburg and Elfman, 2017; Hüssy *et al.*, 2021). It thus seems that the spatial distribution of protein-bound elements like P comply with the hypothesised patterns, with variation between species presumably related to the activity of protein-synthesizing cells in the squamous epithelium (Takagi and Takahashi, 1999).

Randomly trapped and protein-bound: In the present study, concentrations of Mg^{2+} and Mn^{2+} were highest in the distal side of the otolith in both hake and sea bass, with more pronounced asymmetry in hake. 2D maps of Mn only exist previously for *Arapaima* sp., where concentrations are homogenous throughout the otolith (Hüssy *et al.*, 2021) and *Gadus morhua*, where highest concentrations occur in the distal area of the otolith (Limburg *et al.*, 2011; Limburg and Elfman, 2017; Heimbrand *et al.*, 2020; Hüssy *et al.*, 2021). Mg also occurred at higher concentrations along the dorso/ventral growth axis in *Platycephalus bassensis* (McFadden *et al.*, 2016). It thus seems that the spatial patterns in Mg and Mn are also to some degree generic, at least in gadoids. Concentrations are highest in the areas of the otolith dominated by higher concentration of organic matrix, suggesting that the majority of otolith Mg and Mn is protein-bound.

0ther sources of heterogeneity

3D variability: While we treat 2D spatial variation in this study, with a focus towards asymmetric distribution between the proximal and distal sides of the otolith, variability in elemental concentration also occurs in three dimensions. Three dimensional variability of otolith structure is a nascent and promising field of research (e.g. Barry *et al.*, 2008; Palazzo *et al.*, 2022), although variability in 3D otolith chemistry has not yet been treated in the scientific literature, with the implicit assumption, in the absence of further information, that all planes of a sectioned otolith should provide equivalent chemical information. In demonstrating that there is variability in the concentration of elements within a single otolith section, it is logical to suggest that similar variability may occur in three dimensions, for the same reasons as those discussed for a 2D plane. Further studies of chemical composition throughout the structure of the otolith are therefore necessary to aid study design and inter-study comparability.

$CaCO_3$ morph: One major cause of elemental compositional differences within and between otoliths is the form of $CaCO_3$ present in the samples. Significant differences in the concentrations of elements have been found between aragonite, vaterite and calcite (e.g.Pracheil *et al.*, 2017). While aragonite is the most common polymorph of $CaCO_3$ in the sagittal otoliths of Actinopterygian fishes, the vaterite polymorph is found in significantly higher proportions of fishes subjected to stressors (Gauldie 1996; Oxman et al. 2007, Reimer 2017), and is more prevalent in cultured than wild fish otoliths (Reimer *et al.*, 2016; Delaval *et al.*, 2021). Increased prevalence of the calcite polymorph has also been found in some fishes subjected to high pCO_2 (Coll-Lladó *et al.*, 2018; Coll-Lladó *et al.*, 2021), although it is possible that calcite occurrence may be generally under-reported in previous studies (Pracheil *et al.*, 2017), largely due to the difficulties of visual detection (Pracheil *et al.*, 2019). When comparing elemental compositions between polymorphs, numerous studies have found higher concentrations of Ba, K, Na, P, Rb and Sr, and lower concentrations of Al, Mg, Mn and Zn in aragonite than vaterite (Melancon et al., 2009, Veinott et al., 2011, Pracheil et al, 2019, Lewis

et al. 2022, Wood et al., 2022). The biological importance of Mg, Mn, and Zn in protein structures, particularly in enzyme molecules, together with the larger total organic contents in vaterite as opposed to aragonite in conjunction with the larger concentrations of Mn^{2+}, Mg^{2+} and Zn^{2+} ions imply a potential stabilizing role of organic macromolecules and X^{2+} ions for biological vaterite. Thomas *et al.* (2019) also suggest that the increased K concentrations in aragonite over vaterite are due to the complete phosphorylation of the *Stm* protein setting the template for the formation of aragonite instead of vaterite. Additionally, the crystalline structure of vaterite acts to exclude elements such as Ba (Melancon *et al.*, 2009) and grows more rapidly than aragonite, thus creating potential bias towards different periods of incorporation (Tzeng *et al.*, 2007). Calcite has not been well-studied for trace element composition relative to the other, more common morphs, although Pracheil *et al*. (2019) found higher Sr concentration in aragonite than calcite in the otolith of a Chinook salmon *Oncorhynchus tshawytscha* (Walbaum 1792), and Tian *et al.* found higher Sr:Ca and Ba:Ca ratios in aragonite than calcite in juvenile flounder *Paralichthys olivaceus* (Temminck & Schlegel 1846). While Sr may be incorporated relatively homogenously for each accretion of an otolith growth layer, differences in Sr composition between $CaCO_3$ polymorphs have important implications for studies of fishes through otolith chemistry, as Sr concentration is commonly used in tracking migrations, with importance also in spawning physiology (Sturrock *et al.*, 2015).

Temperature and salinity: In general, the elements that have shown relationships with temperature and salinity in their incorporation into fish otoliths are those that do not show proximal-distal asymmetry in distribution (e.g. Ca, Sr, Ba) (e.g. Bath Martin & Wuenschel, 2006, Hüssy *et al.*, 2020). Miller and Hurst (2020) also identified a small, positive effect of temperature on the partition coefficients of both Mg and Mn in otoliths of juvenile *Gadus macrocephalus*, which might suggest an increase in spatial heterogeneity of these elements with increasing temperature due to higher rates of incorporation, or ontogenetic changes with

movements through different water temperatures. Hicks *et al.* (2010) also found relationships between salinity and Li, B, Al, P, S, Mn, Cu, Rb, Sr and Ba in larval *Galaxias maculatus* and *G. argenteus*, with varying signs, again suggesting the potential for variable otolith chemical heterogeneity throughout ontogeny with migration, movements, and differing environmental conditions. It is noteworthy that Ba, Mn, and Mg often show relatively higher concentrations in the central, juvenile portions of the otolith for both species analysed here, indicating potential links with maternal contributions (Thorrold *et al.*, 2006), temperature, or salinity differences in the juvenile life phase (Tian *et al.*, 2021). Mn in both species studied here also shows signs of seasonal or cyclical incorporation, potentially linked to migration between different temperature or salinity regimes or to physiological cycles, but future research in this direction will need to account for the strongly distal asymmetrical distribution of this element throughout the otolith.

Conclusions and perspectives: consequences for otolith microchemistry

Transects and spot samples versus 2D images: This study, investigating the spatial distribution and asymmetry of elemental incorporation throughout the otolith across two species of commercially important fishes, has important implications for the inferences drawn by studies of otolith chemistry. The current standard approaches to the analysis of otolith chemistry are usually transect or spot sampling (e.g. Sturrock *et al.*, 2015; Thomas *et al.*, 2020; Sarakinis *et al.*, 2022). This partial sampling is commonly performed along the longest growth axis of the otolith, between the proximal and distal halves, and carries the risk, unless prior knowledge of elemental spatial distribution is used, of missing the areas of greatest concentrations in asymmetrically distributed elements, or of attributing ecological relevance to the physiological distribution of elements.

Sampling location within an otolith: The choice of location for partial otolith samples is likely, for elements with spatial heterogeneity, to be a major factor in the results of analyses. For protein-bound elements, for example, these may be challenging to detect in the areas of the otolith with lower protein concentrations, such as the translucent winter/slower growth zones. When sampling around the nucleus of the otolith, and during periods of higher growth, however, higher concentrations of protein-bound elements would be expected (Miller et al., 2006; Thomas et al., 2017). Sampling of the proximal or distal halves of the otolith, or sampling positions relative to period of growth will also strongly influence results and their subsequent interpretations for elements with asymmetrical distribution. Indeed, it might be desirable to sample the distal+ and proximal+ elements in their respective regions of prevalence within the otolith. And if, for example, movements are traced through the use of multiple-element fingerprinting with reference to local geochemistry (e.g. Clarke et al., 2015), it may be necessary to design sampling to focus on the otolith zone(s) with prevalence of the elements of interest at the relevant period of growth or to sacrifice precision in favor of sampling the entire life history period of interest (e.g. Marriott *et al.*, 2016; Wright *et al.*, 2018).

Despite the prevalence of location-specific analyses, little attention to date has been given to the elemental spatial heterogeneity across otoliths, thus it remains rare to find chemical composition of otoliths mapped in 2D, and even less common to see inter-species comparisons of these maps. In this study, we have clearly shown spatial heterogeneity and asymmetry between elements and between species. We have also demonstrated general trends in the spatial distribution patterns of many commonly analyzed elements. Understanding the processes of biomineralization for different elements is therefore essential for reliable measurement and interpretation in otolith microchemistry studies. A location-specific approach to otolith elemental chemistry, without prior knowledge of or accounting for elemental heterogeneity or patterns, may lead to biased or missing information when comparing between studies, species,

or locations (e.g. Melancon *et al.*, 2009; Chang and Geffen, 2013; Hüssy *et al.*, 2021). The patterns shown here of elemental distribution based on the cellular architecture of the saccular epithelium, substitution for Ca2+, protein distribution, or random trapping of the elements are important for the design of future studies, and for comparison with existing studies. We demonstrate the crucial role of accounting for spatial heterogeneity in otolith chemical composition, by 2D (and, in the future, possibly 3D) mapping of the sampling area and relevant spatial analyses, to understand the implications of elemental entrainment and concentration in otoliths for interpretation of biological and environmental signals, and to enable robust comparison and inferences in elemental studies.

Acknowledgments

We thank Emilie Le Luherne (Ifremer) who prepared the sea bass otoliths and Gaëlle Barbotin (UMR 5254) for running the ICPMS analyses. We also thank the editor and two anonymous reviewers for their comments, which have greatly improved this manuscript.

Author Contributions

H.P.: conceptualization, investigation, project administration, writing, review and editing; K.M.M., H.T., F.D., K.M., C.P., K.H.: investigation, writing, review and editing.

References

Alvarez, P., Motos, L., Uriarte, A., and Egaña, J. 2001. Spatial and temporal distribution of European hake, *Merluccius merluccius* (L.), eggs and larvae in relation to hydrographical conditions in the Bay of Biscay. Fisheries Research, 50: 111–128.

Asano, M. & Mugiya, Y. (1993). BIOCHEMICAL AND CALCIUM-BINDING PROPERTIES OF WATER-SOLUBLE PROTEINS ISOLATED FROM OTOLITHS OF THE TILAPIA, ORECHROMIS-NILOTICUS. *Comparative Biochemistry and Physiology B-Biochemistry & Molecular Biology* **104**, 201-205.

Baba, K., Shimizu, M., Mugiya, Y. & Yamada, J. (1991). Otolith Matrix Proteins of Walleye Pollock; Biochemical Properties and Immunohistochemical Localization in the Saccular Tissue. pp. 57-61. Tokyo: Springer Japan.

Barry, B., Markwitz, A. & David, B. (2008). THREE DIMENSIONAL IMAGING OF OTOLITHS. *International Journal of PIXE* **18**, 131-137.

Bath Martin, G., & Wuenschel, M. J. (2006). Effect of Temperature and Salinity on Otolith Element Incorporation in Juvenile Gray Snapper *Lutjanus griseus*. *Marine Ecology Progress Series* 324: 229–39. https://doi.org/10.3354/meps324229.

Beier, M., Anken, R. & Hilbig, R. (2006). Sites of calcium uptake of fish otoliths correspond with macular regions rich of carbonic anhydrase. *Advances in Space Research* **38**, 1123-1127.

Beier, M., Anken, R. H. & Rahmann, H. (2004). Calcium-tracers disclose the site of biomineralization in inner ear otoliths of fish. In *Space Life Sciences: Search for Signatures of Life, and Space Flight Environmental Effects on the Nervous System* (Horneck, G., LevasseurRegourd, A. C., Rabin, B. M. & Slenzka, K. B., eds.), pp. 1401-1405.

Borelli, G., Mayer-Gostan, N., Merle, P. L., De Pontual, H., Boeuf, G., Allemand, D. & Payan, P. (2003). Composition of biomineral organic matrices with special emphasis on turbot (*Psetta maxima*) otolith and endolymph. *Calcified Tissue International* **72**, 717-725.

Chang, M.-Y. & Geffen, A. J. (2013). Taxonomic and geographic influences on fish otolith microchemistry. *Fish and Fisheries* **14**, 458-492.

Clarke, A. D., Telmer, K. H. & Shrimpton, J. M. (2015). Movement Patterns of Fish Revealed by Otolith Microchemistry: A Comparison of Putative Migratory and Resident Species. *Environmental Biology of Fishes* **98**, 1583–97. https://doi.org/10.1007/s10641-015-0384-6

Coll-Lladó, C., Giebichenstein, J., Webb, P. B., Bridges, C. R. & de la serrana, D. G. (2018). Ocean acidification promotes otolith growth and calcite deposition in gilthead sea bream (*Sparus aurata*) larvae. *Scientific Reports* **8**, 8384.

Coll-Lladó, C., Mittermayer, F., Webb, P. B., Allison, N., Clemmesen, C., Stiasny, M., Bridges, C. R., Göttler, G. & Garcia de la serrana, D. (2021). Pilot study to investigate the effect of long-term exposure to high pCO2 on adult cod (*Gadus morhua*) otolith morphology and calcium carbonate deposition. *Fish Physiology and Biochemistry* **47**, 1879-1891.

Collingsworth, P. D., Van Tassell, J. J., Olesik, J. W. & Marschall, E. A. (2010). Effects of temperature and elemental concentration on the chemical composition of juvenile

yellow perch (*Perca flavescens*) otoliths. *Canadian Journal of Fisheries and Aquatic Sciences* **67**, 1187-1196.

Cruz, S., Shiao, J. C., Liao, B. K., Huang, C. J. & Hwang, P. P. (2009). Plasma membrane calcium ATPase required for semicircular canal formation and otolith growth in the zebrafish inner ear. *Journal of Experimental Biology* **212**, 639-647.

de Pontual, H., Heerah, K., Goossens, J., Garren, F., Martin, S., Le Ru, L., Le Roy, D., & Woillez, M. (2023) Seasonal migration, site fidelity, and population structure of European seabass (*Dicentrarchus labrax*). *ICES Journal of Marine Science*, fsad087. https://doi.org/10.1093/icesjms/fsad087.

De Pontual, H., A. Jolivet, M. Bertignac, and R. Fablet. 'Diel Vertical Migration of European Hake Merluccius Merluccius and Associated Temperature Histories: Insights from a Pilot Data-Storage Tagging (DST) Experiment'. *Journal of Fish Biology* 81, no. 2 (2012): 728–34. https://doi.org/10.1111/j.1095-8649.2012.03345.x.

de Pontual, H., Jolivet, A., Garren, F. & Bertignac, M. (2013). New insights on European hake biology and population dynamics from a sustained tagging effort in the Bay of Biscay. *Ices Journal of Marine Science* **70**, 1416-1428.

Delaval, A., Solås, M. R., Skoglund, H. & Salvanes, A. G. V. (2021). Does Vaterite Otolith Deformation Affect Post-Release Survival and Predation Susceptibility of Hatchery-Reared Juvenile Atlantic Salmon? *Frontiers in Veterinary Science* **8**.

Doubleday, Z. A., Harris, H. H., Izzo, C. & Gillanders, B. M. (2014). Strontium Randomly Substituting for Calcium in Fish Otolith Aragonite. *Analytical Chemistry* **86**, 865-869.

Edeyer, A., de Pontual, H., Payan, P., Troadec, H., Severe, A. & Mayer-Gostan, N. (2000). Daily variations of the saccular endolymph and plasma compositions in the turbot *Psetta maxima*: relationship with the diurnal rhythm in otolith formation. *Marine Ecology Progress Series* **192**, 287-294.

Heimbrand, Y., Limburg, K. E., Hussy, K., Casini, M., Sjoberg, R. R., Bratt, A. M. P. & Ohlund, J. (2020). Seeking the true time: Exploring otolith chemistry as an aage-determination tool (vol 97, pg 552, 2020). *Journal of Fish Biology* **97**, 1291-1291.

Hicks, A. S., Closs, G. P. & Swearer, S. E. (2010). Otolith Microchemistry of Two Amphidromous Galaxiids across an Experimental Salinity Gradient: A Multi-Element Approach for Tracking Diadromous Migrations. *Journal of Experimental Marine Biology and Ecology* 394: 86–97. https://doi.org/10.1016/j.jembe.2010.07.018.

Hüssy, K., Limburg, K. E., de Pontual, H., Thomas, O. R. B., Cook, P. K., Heimbrand, Y., Blass, M. & Sturrock, A. M. (2021). Trace Element Patterns in Otoliths: The Role of Biomineralization. *Reviews in Fisheries Science & Aquaculture* **29**, 445-477.

Izzo, C., Doubleday, Z. A. & Gillanders, B. M. (2016). Where do elements bind within the otoliths of fish? *Marine and Freshwater Research* **67**, 1072-1076.

Kwan, G. T., Smith, T. R. & Tresguerres, M. (2020). Immunological characterization of two types of ionocytes in the inner ear epithelium of Pacific Chub Mackerel (*Scomber japonicus*). *Journal of Comparative Physiology B-Biochemical Systems and Environmental Physiology* **190**, 419-431.

Le Luherne, E., Daverat, F., Woillez, M., Pécheyran, C., & de Pontual, H. (2022). Coupling natural and electronic tags to explore spawning site fidelity and natal homing in northeast Atlantic European seabass. *Estuarine, Coastal and Shelf Science*, ***278***, 108118.

Limburg, K. E. & Elfman, M. (2017). Insights from two-dimensional mapping of otolith chemistry. *Journal of Fish Biology* **90**, 480-491.

Limburg, K. E., Lochet, A., Driscoll, D., Dale, D. S. & Huang, R. (2010). Selenium detected in fish otoliths: a novel tracer for a polluted lake? *Environmental Biology of Fishes* **89**, 433-440.

Limburg, K. E., Olson, C., Walther, Y., Dale, D., Slomp, C. P. & Hoie, H. (2011). Tracking Baltic hypoxia and cod migration over millennia with natural tags. *Proceedings of the National Academy of Sciences of the United States of America* **108**, E177-E182.

Limburg, K. E., Walther, B. D., Lu, Z. L., Jackman, G., Mohan, J., Walther, Y., Nissling, A., Weber, P. K. & Schmitt, A. K. (2015). In search of the dead zone: Use of otoliths for tracking fish exposure to hypoxia. *Journal of Marine Systems* **141**, 167-178.

López, R., Pontual, H. de, Bertignac, M., & Mahévas, S. 2015. What can exploratory modelling tell us about the ecobiology of European sea bass (*Dicentrarchus labrax*): a comprehensive overview. Aquatic Living Resources, 28: 61–79. EDP Sciences.

Marriott, A. L., McCarthy, I. D., Ramsay, A. L. & Chenery, S. R. N. (2016). Discriminating nursery grounds of juvenile plaice (*Pleuronectes platessa*) in the south-eastern Irish Sea using otolith microchemistry. *Marine Ecology Progress Series* **546**, 183-195.

MayerGostan, N. (1997). Distribution of ionocytes in the saccular epithelium of the inner ear of two teleosts (*Oncorhynchus mykiss* and *Scophthalmus maximus*). *Cell and Tissue Research* **289**, 53-61.

McFadden, A., Wade, B., Izzo, C., Gillanders, B. M., Lenehan, C. E. & Pring, A. (2016). Quantitative electron microprobe mapping of otoliths suggests elemental incorporation is affected by organic matrices: implications for the interpretation of otolith chemistry. *Marine and Freshwater Research* **67**, 889-898.

Melancon, S., Fryer, B. J. & Markham, J. L. (2009). Chemical Analysis of Endolymph and the Growing Otolith: Fractionation of Metals in Freshwater Fish Species. *Environmental Toxicology and Chemistry* **28**, 1279-1287.

Miller, J. A., & Hurst, T. P. 'Growth Rate, Ration, and Temperature Effects on Otolith Elemental Incorporation'. *Frontiers in Marine Science* 7 (2020). https://www.frontiersin.org/articles/10.3389/fmars.2020.00320.

Miller, M. B., Clough, A. M., Batson, J. N. & Vachet, R. W. (2006). Transition metal binding to cod otolith proteins. *Journal of Experimental Marine Biology and Ecology* **329**, 135-143.

Mugiya, Y. & Uchimura, T. (1989). Otolith resorption induced by anaerobic stress in the goldfish, *Carassius auratus Journal of Fish Biology* **35**, 813-818.

Murayama, E., Takagi, Y. & Nagasawa, H. (2004). Immunohistochemical localization of two otolith matrix proteins in the otolith and inner ear of the rainbow trout, *Oncorhynchus mykiss*: comparative aspects between the adult inner ear and embryonic otocysts. *Histochemistry and Cell Biology* **121**, 155-166.

Palazzo, Q., Stagioni, M., Raaijmakers, S., Belleman, R. G., Prada, F., Hammel, J. U., Fermani, S., Kaandorp, J., Goffredo, S. & Falini, G. (2022). Multiscale analysis on otolith structural features reveals differences in ontogenesis and sex in *Merluccius merluccius* in the western Adriatic Sea. *Royal Society Open Science* **9**, 211943.

Panfili, J., de Pontual, H., Troadec, H. & P.J., W., eds. (2002). *Manual of fish sclerochronology*: Ifremer- IRD coedition, Brest, France, 464 p.

Pawson, M. G., & Pickett, G. D. (1996). The Annual Pattern of Condition and Maturity in Bass, *Dicentrarchus labrax*, in Waters Around England and Wales. *Journal of the Marine Biological Association of the United Kingdom*, *76*, 107–125.

Payan, P., Borelli, G., Priouzeau, F., De Pontual, H., Boeuf, G. & Mayer-Gostan, N. (2002). Otolith growth in trout *Oncorhynchus mykiss*: supply of Ca2+ and Sr2+ to the saccular endolymph. *Journal of Experimental Biology* **205**, 2687-2695.

Payan, P., De Pontual, H., Boeuf, G. & Mayer-Gostan, N. (2004). Endolymph chemistry and otolith growth in fish. *Comptes Rendus Palevol* **3**, 535-547.

Payan, P., Edeyer, A., De Pontual, H., Borelli, G., Boeuf, G. & Mayer-Gostan, N. (1999). Chemical composition of saccular endolymph and otolith in fish inner ear: lack of spatial uniformity. *American Journal of Physiology-Regulatory Integrative and Comparative Physiology* **277**, R123-R131.

Pisam, M., Payan, P., LeMoal, C., Edeyer, A., Boeuf, G. & Mayer-Gostan, N. (1998). Ultrastructural study of the saccular epithelium of the inner ear of two teleosts, *Oncorhynchus mykiss* and *Psetta maxima*. *Cell and Tissue Research* **294**, 261-270.

Poulard, J.-C. (2001). Distribution of hake (*Merluccius merluccius*, Linnaeus, 1758) in the Bay of Biscay and the Celtic sea from the analysis of French commercial data. *Fisheries Research*, *50*, 173–187.

Pracheil, B. M., Chakoumakos, B. C., Feygenson, M., Whitledge, G. W., Koenigs, R. P. & Bruch, R. M. (2017). Sturgeon and paddlefish (Acipenseridae) sagittal otoliths are composed of the calcium carbonate polymorphs vaterite and calcite. *Journal of Fish Biology* **90**, 549-558.

Pracheil, B. M., George, R. & Chakoumakos, B. C. (2019). Significance of otolith calcium carbonate crystal structure diversity to microchemistry studies. *Reviews in Fish Biology and Fisheries* **29**, 569-588.

Prohaska, T., Irrgeher, J. & Zitek, A. (2016). Simultaneous multi-element and isotope ratio imaging of fish otoliths by laser ablation split stream ICP-MS/MC ICP-MS. *Journal of Analytical Atomic Spectrometry* **31**, 1612-1621.

Reimer, T., Dempster, T., Warren-Myers, F., Jensen, A. J. & Swearer, S. E. (2016). High prevalence of vaterite in sagittal otoliths causes hearing impairment in farmed fish. *Scientific Reports* **6**, 25249.

Rueden, C. T.; Schindelin, J. & Hiner, M. C. et al. (2017). ImageJ2: ImageJ for the next generation of scientific image data. *BMC Bioinformatics* **18**, 529, doi:10.1186/s12859-017-1934-z

Sarakinis, K. G., Taylor, M. D., Johnson, D. D. & Gillanders, B. M. (2022). Determining population structure and connectivity through otolith chemistry of stout whiting, *Sillago robusta*. *Fisheries Management and Ecology* **29**, 760-773.

Sasagawa, T. & Mugiya, Y. (1996). Biochemical properties of water-soluble otolith proteins and the immunobiochemical detection of the proteins in serum and various tissues in the Tilapia *Oreochromis niloticus*. *Fisheries Science* **62**, 970-976.

Schulz-Mirbach, T., Ladich, F., Plath, M. & Hess, M. (2019). Enigmatic ear stones: what we know about the functional role and evolution of fish otoliths. *Biological Reviews* **94**, 457-482.

Shiao, J. C., Lin, L. Y., Horng, J. L., Hwang, P. P. & Kaneko, T. (2005). How can teleostean inner ear hair cells maintain the proper association with the accreting otolith? *Journal of Comparative Neurology* **488**, 331-341.

Staby, A., Skjæraasen, J. E., Geffen, A. J., & Howell, D. (2018). Spatial and temporal dynamics of European hake (*Merluccius merluccius*) in the North Sea. *ICES Journal of Marine Science*, *75*, 2033–2044.

Sturrock, A. M., Hunter, E., Milton, J. A., Johnson, R. C., Waring, C. P., Trueman, C. N. & Eimf (2015). Quantifying physiological influences on otolith microchemistry. *Methods in Ecology and Evolution* **6**, 806-816.

Sturrock, A. M., Trueman, C. N., Milton, J. A., Waring, C. P., Cooper, M. J. & Hunter, E. (2014). Physiological influences can outweigh environmental signals in otolith microchemistry research. *Marine Ecology Progress Series* **500**, 245-264.

Takagi, Y. (1997). Meshwork arrangement of mitochondria-rich, Na+,K+-ATPase-rich cells in the saccular epithelium of rainbow trout (*Oncorhynchus mykiss*) inner ear. *Anatomical Record* **248**, 483-489.

Takagi, Y. & Takahashi, A. (1999). Characterization of ootolith soluble-matrix producing cells in the saccular epithelium of rainbow trout (*Oncorhynchus mykiss*) inner ear. *Anat Rec* **254**, 322-329.

Tanner, S. E., Vasconcelos, R. P., Cabral, H. N., & Thorrold, S. R. (2012). Testing an otolith geochemistry approach to determine population structure and movements of European hake in the northeast Atlantic Ocean and Mediterranean Sea. *Fisheries Research*, *125–126*, 198–205.

Thomas, O. R. B., Ganio, K., Roberts, B. R. & Swearer, S. E. (2017). Trace element-protein interactions in endolymph from the inner ear of fish: implications for environmental reconstructions using fish otolith chemistry. *Metallomics* **9**, 239-249.

Thomas, O. R. B. & Swearer, S. E. (2019). Otolith Biochemistry-A Review. *Reviews in Fisheries Science & Aquaculture* **27**, 458-489.

Thomas, O. R. B., Swearer, S. E., Kapp, E. A., Peng, P., Tonkin-Hill, G. Q., Papenfuss, A., Roberts, A., Bernard, P. & Roberts, B. R. (2019). The inner ear proteome of fish. *Febs Journal* **286**, 66-81.

Thomas, O. R. B., Thomas, K. V., Jenkins, G. P. & Swearer, S. E. (2020). Spatio-temporal resolution of spawning and larval nursery habitats using otolith microchemistry is element dependent. *Marine Ecology Progress Series* **636**, 169-187.

Thorrold, S. R., Jones, G. P., Planes, S., & Hare, J. A. (2006). Transgenerational marking of embryonic otoliths in marine fishes using barium stable isotopes. *Canadian Journal of Fisheries and Aquatic Sciences*, *63*, 1193–1197.

Tian, H., Liu, J., Cao, L., & Dou, S. (2021). Temperature and salinity effects on strontium and barium incorporation into otoliths of flounder *Paralichthys olivaceus* at early life stages. *Fisheries Research*, *239*, 105942.

Tohse, H., Ando, H. & Mugiya, Y. (2004). Biochemical properties and immunohistochemical localization of carbonic anhydrase in the sacculus of the inner ear in the salmon *Oncorhynchus masou*. *Comparative Biochemistry and Physiology a-Molecular & Integrative Physiology* **137**, 87-94.

Tohse, H. & Mugiya, Y. (2001). Effects of enzyme and anion transport inhibitors on in vitro incorporation of inorganic carbon and calcium into endolymph and otoliths in salmon *Oncorhynchus masou*. *Comparative Biochemistry and Physiology a-Molecular and Integrative Physiology* **128**, 177-184.

Tzeng, W. N., Chang, C. W., Wang, C. H., Shiao, J. C., Iizuka, Y., Yang, Y. J., You, C. F. & Lozys, L. (2007). Misidentification of the migratory history of anguillid eels by Sr/Ca ratios of vaterite otoliths. *Marine Ecology Progress Series* **348**, 285-295.

Vieira, F. A., Gregorio, S. F., Ferraresso, S., Thorne, M. A. S., Costa, R., Milan, M., Bargelloni, L., Clark, M. S., Canario, A. V. M. & Power, D. M. (2011). Skin healing and scale regeneration in fed and unfed sea bream, *Sparus auratus*. *Bmc Genomics* **12**.

Walther, B. D. (2019). The art of otolith chemistry: interpreting patterns by integrating perspectives. *Marine and Freshwater Research* **70**, 1643-1658.

Weigele, J., Franz-Odendaal, T. A. & Hilbig, R. (2015). Spatial Expression of Otolith Matrix Protein-1 and Otolin-1 in Normally and Kinetotically Swimming Fish. *Anatomical Record-Advances in Integrative Anatomy and Evolutionary Biology* **298**, 1765-1773.

Wright, P. J., Régnier, T., Gibb, F. M., Augley, J. & Devalla, S. (2018). Assessing the role of ontogenetic movement in maintaining population structure in fish using otolith microchemistry. *Ecology and Evolution* **8**, 7907-7920.

Wyndham, T., McCulloch, M., Fallon, S., Alibert, C. (2004). High resolution coral records of rare earth elements in coastal seawater: biogeochemical cycling and a new environmental proxy. *Geochimica et Cosmochimica Acta* **68**, 2067-2080.